

Solution and Solid-State Study of Heteroleptic Hg(II)-Thiolates: Crystal Structures of $[\text{Hg}_4\text{I}_4(\text{SCH}_2\text{CH}_2\text{NH}_2)_4]$ and $[\text{Hg}_4\text{I}_8(\text{SCH}_2\text{CH}_2\text{NH}_3)_2]_n \cdot n\text{H}_2\text{O}$

Mohan S. Bharara, Sean Parkin, and David A. Atwood*

Department of Chemistry, University of Kentucky, Lexington, Kentucky 40506-0055

Received November 17, 2005

Combination of 2-aminoethanethiol hydrochloride and HgI_2 in water in the presence of a base yielded a cyclic molecular structure, $[\text{Hg}_4\text{I}_4(\text{SCH}_2\text{CH}_2\text{NH}_2)_4]$ (**1**). For the same reaction in the absence of the base, a similar structure with protonated amines was expected; however, polymeric $[\text{Hg}_4\text{I}_8(\text{SCH}_2\text{CH}_2\text{NH}_3)_2]_n \cdot n\text{H}_2\text{O}$ (**2**) was formed instead. The structures are quite variable despite similar reaction conditions. For instance, there is an additional Hg–N interaction in **1** due to the use of base. The environment around tetracoordinate Hg in **1** is comprised of S, N, and I atoms, with the ligand forming a five-membered chelate and the I atoms present alternate to each other. In the repeating unit of **2**, three independent types of Hg atoms are observed, with HgI_3 , HgS_2I_2 , and HgI_4 bonding environments that have both bridging and terminal I atoms. A simple mechanistic pathway for the formation of **1** and **2** is proposed that includes the presence of three- and four-coordinate Hg intermediates in the solution. Intermolecular hydrogen bonding involving N, I, and S in **1** and N, I, and O atoms in **2** create extended three-dimensional networks. The shortest Hg···Hg distances are found to be intrachain in the range 3.938–3.962 Å and indicate no interaction between these atoms. The solution studies (UV–vis and NMR) along with solid-state (IR, Raman, and X-ray) studies for **1** and **2** confirm retention of the structural configuration in the solution. The thermal study of **2** indicates that degradation of the complex occurs in a single step, in contrast to **1**, which takes a more complicated decomposition pathway.

Introduction

There is an immense interest in the structural chemistry of mercury(II)-thiolates to understand mercury–cysteine interactions in biological systems and also as precursors to solid-state materials.^{1–3} The Hg(II)-thiolates are well-known for their unusual coordination environment and exhibit structural variability in both the solution and solid states. Despite the thermodynamically favorable Hg–S bond, a number of structures of equal energy with varying geometry around the Hg atom are typically observed.⁴ The variable structures are often derivative of linear two-coordinate compounds.⁵ For instance, homoleptic Hg(II)-thiolates adopt discrete molecular ($[\text{Hg}_x(\text{SR})_y]$) ($x = 1–5$ and $y = 2–8$) as

well as polymeric ($[\text{Hg}(\text{SR})_2]_\infty$ and $[\text{Hg}_2(\text{SR})_3]_\infty$) structures.^{6–9} On the other hand, heteroleptic thiolates containing both monodentate thiolate and halide are generally nonmolecular and may be one-dimensional ($[\text{Hg}(\text{SR})\text{Cl}]_\infty$ and $[\text{HgS}(\text{steroid})\text{Br}]_\infty$) or two-dimensional ($[\text{Hg}(\text{SMe})\text{X}]_\infty$ ($\text{X} = \text{Cl}$ or Br) and $[\text{Hg}(\text{SP}^i)\text{Cl}]_\infty$) polymers.^{10–12} Molecular structures of higher nuclearity are not very common but include compounds such as $(\text{Ph}_4\text{P})[(\mu\text{-SEt})_5(\mu\text{-Br})(\text{HgBr})_4]$, $(\text{Et}_4\text{N})_2[(\mu\text{-I})(\mu\text{-SP}^i)(\text{HgI}_2)_2]$, $(\text{Bu}^n_4\text{N})_2[\text{Hg}_4(\text{SR})_6\text{X}_4]$ ($\text{R} = \text{SEt}$ and SP^i), $[\text{Hg}_4\{\text{S}(\text{CH}_2)_2\text{NMe}_2\}_4\text{X}_4]$ and $[\text{Hg}_7(\text{SC}_6\text{H}_{11})_{12}\text{X}_2]$ ($\text{X} = \text{Cl}$, Br or I).^{10,13,14}

* To whom correspondence should be addressed. E-mail: datwood@uky.edu.

- (1) Blower, P. J.; Dilworth, J. R. *Coord. Chem. Rev.* **1987**, *76*, 121–185.
- (2) Dance, I. G. *Polyhedron* **1986**, *5*, 1037.
- (3) Henkel, G.; Krebs, B. *Chem. Rev.* **2004**, *104*, 801.
- (4) Govindaswamy, N.; Moy, J.; Millar, M.; Koch, S. A. *Inorg. Chem.* **1992**, *31*, 5343.
- (5) Wright, J. G.; Natan, M. J.; MacDonnell, F. M.; Ralston, D. M.; O'Halloran, T. V. *Prog. Inorg. Chem.* **1990**, *29*, 323.

- (6) Bowmaker, G. A.; Dance, I. G.; Dobson, B. C.; Roger, D. A. *Aust. J. Chem.* **1984**, *37*, 1607.
- (7) Henkel, G.; Betz, P.; Krebs, B. *Chem. Commun.* **1985**, *21*, 1498.
- (8) Henkel, G.; Betz, P.; Krebs, B. *Inorg. Chim. Acta* **1987**, *134*, 195.
- (9) Krauter, G.; Neumuller, B.; Goedken, V. L.; Rees, W. S. *Chem. Mater.* **1996**, *8*, 360.
- (10) Casals, I.; Gonzalez-Duarte, P.; Sola, J.; Miravittles, C.; Molins, E. *Polyhedron* **1988**, *7*, 2509.
- (11) Canty, A. J.; Raston, C. L.; White, A. H. *Aust. J. Chem.* **1979**, *32*, 311.
- (12) Biscarini, P.; Foresti, E.; Paradella, G. *J. Chem. Soc., Dalton Trans.* **1984**, 953.
- (13) Alsina, T.; Clegg, W.; Fraser, K. A.; Sola, J. *Chem. Commun.* **1992**, *14*, 1010.

For heteroleptic Hg(II)-thiolates, it is generally observed that the structure (molecular or nonmolecular) associated with the compounds is independent of the type of halide present.^{13,15–19} However, the geometry around Hg is affected by the type of halide. For instance, in [Hg(SR)₂X₂] compounds, the deviation from ideal tetrahedral geometry is more noticeable for Cl and Br than for I. The pronounced distortion may be due to a vibronic coupling mechanism leading to the d-orbital contribution in the bond.²⁰ The deformation for distorted tetrahedral Hg(II)-alkenethiolates is greatest for the Cl derivative, which has the smallest difference in donor strength between halide and sulfur.⁴ Earlier, we reported the formation of linear as well as discrete molecular compounds from a combination of HgX₂ (X = Cl, Br) and 2-aminoethanethiol.^{21,22} In [Hg₆Cl₈(SCH₂CH₂NH₃)₈]⁴⁺ and [Hg₉Br₁₅(SCH₂CH₂NH₃)₉]³⁺, it is observed that the halide (Cl and Br, respectively) is responsible for the clusters observed.²² In an effort to understand the effect of the iodide ions, we report here novel [Hg₄I_x(SR)_y] (tetra- and polynuclear) compounds obtained by the combination of HgI₂ and 2-aminoethanethiol hydrochloride. Plausible mechanistic pathways for the formation of **1** and **2** are also reported and implicate three- and four-coordinate Hg complexes in the solution.

Experimental Section

General Procedure. The reactions were carried out at room temperature in a mixture of DI water and methanol under nitrogen. The reagents 2-aminoethanethiol hydrochloride (TCI America) and HgI₂ (Alfa Aesar) were used as received. ¹H and ¹³C NMR data were obtained with JEOL-GSX-400 and 270 instruments operating at 199.17 MHz using *d*₆-DMSO as solvent. The ¹⁹⁹Hg{¹H} NMR spectrum of **1** (0.5M) in *d*₆-DMSO was collected at 25 °C on a Varian INOV 400 MHz instrument with 4-Nucleus Autoswitchable 5 mm Probe; data were referenced to 1 M HgCl₂ in DMSO at –1500 ppm^{23,24} and checked against external 0.1 M Hg(ClO₄)₂ in D₂O (–2250 ppm).²⁵ The IR data were recorded as KBr pellets on a Mattson Galaxy 5200 FT-IR instrument between 400 and 4000 cm⁻¹. Mass spectral data (MALDI) were obtained on a Kratos Kompact SEQ MALDI-TOFMS at the University of Kentucky Mass Spectrometry Facility. Raman spectra were obtained on a Nicolet FT-Raman 906 Spectrometer ESP between 100 and 800 cm⁻¹ at

the Center for Applied Energy Research at the University of Kentucky facility. The UV–vis studies were conducted on an Agilent HP 8453 instrument by using 0.05 mM solutions of **1** and **2** in an 80:20 v/v water:DMSO mixture. The thermogravimetric analyses were done on a DSC 2950 thermal analyzer with a TGA 2950 furnace operating at 10 °C/min in an open atmosphere.

X-ray Crystallography. Crystals of **1** and **2** were obtained in high yield by two methods: the partial evaporation of the filtrate and recrystallization in DI water. Crystals obtained by partial evaporation were used for the x-ray study. X-ray diffraction data were collected at 90 and 173 K on a Nonius Kappa CCD diffractometer unit using Mo–Kα radiation from regular-shaped crystals mounted in Paratone-*N* oil on glass fibers. Initial cell parameters were obtained using DENZO²⁶ from 1° frames and were refined via a least-squares scheme using all data-collection frames (SCALEPACK).²⁶ The structures were solved by direct methods (SHELXL97)²⁷ and completed by difference Fourier methods (SHELXL97).²⁷ Refinement was performed against *F*² by weighted full-matrix least-squares, and an empirical absorption correction (SADABS²⁷) was applied. Hydrogen atoms were placed at calculated positions using suitable riding models with isotropic displacement parameters derived from their carrier atoms. Non-hydrogen atoms were refined with anisotropic displacement parameters. Atomic scattering factors were taken from the International Tables for Crystallography Volume C.²⁸ Crystal data, selected bond distances, and angles are provided in Tables 1–3.

Synthesis of [Hg₄I₄(SCH₂CH₂NH₂)₄] (1**).** To a stirring solution of 2-aminoethanethiol hydrochloride (10 mmol, 1.14 g) and NaOH (10 mmol, 0.4 g) in a mixture of DI water (90 mL) and methanol (10 mL) was added HgI₂ (5 mmol, 2.27 g), and the solution was stirred for 3 days. The precipitate was removed, washed with methanol followed by cold water, and vacuum-dried. Evaporation of the filtrate at room temperature yielded X-ray quality crystals. Crystals could also be obtained by recrystallization of the precipitate in DI water. Yield (crystals + precipitate): 2.5 g (62%). Mp: 175–177°. ¹H NMR (*d*₆-DMSO, 200 MHz): δ 2.84 (t, 2H, SCH₂), 2.96 (t, 2H, NCH₂), 6.06 (br, 2H, NH₂). ¹³C NMR (*d*₆-DMSO, 200 MHz): δ 29.1 (CH₂S), 42.7 (CH₂N). ¹⁹⁹Hg{¹H} NMR (*d*₆-DMSO, 400 MHz): δ –642. IR (KBr, ν (cm⁻¹)): 3445, 3164, 2831, 1601, 1555, 1364, 1266, 1153, 1018, 935, 630. MALDI MS (*m/z* (%)): 356 ([Hg(SCH₂CH₂NH₂)₂]⁺, 5), 401 ([HgI(SCH₂CH₂NH₂)]⁺, 5), 146 ([NH₄I]⁺, 25), 172 ([CH₂CH₂NH₃I]⁺, 100), 78 ([SCH₂CH₂NH₂]⁺, 47). Anal. Calcd for [Hg₄I₄(SCH₂CH₂NH₂)₄]: C, 5.951; H, 1.498; N, 3.470. Found: C, 5.949; H, 1.486; N, 3.481.

Synthesis of [Hg₄I₈(SCH₂CH₂NH₃)₂]_n·nH₂O (2**).** To a stirring solution of 2-aminoethanethiol hydrochloride (10 mmol, 1.14 g) in a mixture of DI water (90 mL) and methanol (10 mL) was added HgI₂ (5 mmol, 2.27 g), and the solution was stirred for 3 days. The precipitate was removed, washed with methanol followed by cold water, and vacuum-dried. Evaporation of the filtrate at room temperature yielded X-ray quality crystals. Crystals could also be obtained by recrystallization of the precipitate in DI water. Yield (crystals + precipitate): 4.03 g (80%). Mp: 110–112°. ¹H NMR (*d*₆-DMSO, 200 MHz): δ 3.04 (m, 4H, SCH₂ and NCH₂), 7.68 (br, 3H, NH₃). ¹³C NMR (*d*₆-DMSO, 200 MHz): δ 27.3 (CH₂S), 42.5 (CH₂N). IR (KBr, ν (cm⁻¹)): 3720, 3448, 3164, 2962, 2831, 1594, 1468, 1407, 1364, 1260, 1086, 804, 675. MALDI MS (*m/z* (%)): 172 ([CH₂CH₂NH₃I]⁺, 100), 144 ([NH₄I]⁺, 7). Anal. Calcd

- (14) Dean, P. A.; Jagadese, J. V.; Wu, Y. *Inorg. Chem.* **1994**, *33*, 2180.
 (15) Bermejo, E.; Castineiras, A.; Garcia, I.; West, D. X. *Polyhedron* **2003**, *22*, 1147.
 (16) Bell, N. A.; Coles, S. J.; Constable, C. P.; Hibbs, D. E.; Hursthouse, M. B.; Mansor, R.; Raper, E. S.; Sammon, C. *Inorg. Chim. Acta* **2001**, *323*, 69.
 (17) Bell, N. A.; Branston, T. N.; Clegg, W.; Creighton, J. R.; Cucurull-Sanchez, L.; Elsegood, R. J. M.; Raper, E. S. *Inorg. Chim. Acta* **2000**, *303*, 220.
 (18) Stalhandske, C. M. V.; Persson, I.; Sandstrom, M.; Aberg, M. *Inorg. Chem.* **1997**, *36*, 4945.
 (19) Taylor, N. J.; Carty, A. J. *J. Am. Chem. Soc.* **1977**, *99*, 6143.
 (20) Bersuker, I. B. *Electronic Structure and Properties of Transition Metal Compounds*; Wiley-Interscience: New York, 1996.
 (21) Kim, C. H.; Parkin, S.; Bharara, M. S.; Atwood, D. A. *Polyhedron* **2002**, *21*, 225.
 (22) Bharara, M. S.; Bui, T. H.; Parkin, S.; Atwood, D. A. *Inorg. Chem.* **2005**, *44*, 5753.
 (23) Sens, M. A.; Wilson, N. K.; Ellis, P. D.; Odon, J. D. *J. Magn. Reson.* **1975**, *19*, 323.
 (24) Al-Showiman, S. S. *Inorg. Chim. Acta* **1988**, *141*, 263.
 (25) Pregosin, P. S. *Transition Metal Nuclear Magnetic Resonances*; Elsevier: New York, 1991.

- (26) Otwinowski, Z.; Moinor, W. *Methods Enzymol.* **1997**, *276*, 307.
 (27) Sheldrick, G. M. *SADABS, an Empirical Adsorption Correction Program*; Bruker Analytical X-ray Systems: Madison, WI, 1996.
 (28) *International Tables for Crystallography, Vol. C*; Kluwer Academic Publishers: Dordrecht, The Netherlands, 1992.

Table 1. Crystal Data for **1** and **2**

	1	2
empirical formula	C ₄ H ₁₂ Hg ₂ I ₂ N ₂ S ₂	C ₂ H ₆ Hg ₂ I ₄ NOS
fw	807.26	1003.94
<i>T</i> (K)	90.0(2)	90.0(2)
wavelength (Å)	0.71073	0.71073
cryst syst	monoclinic	orthorhombic
space group	<i>P</i> 2 ₁ / <i>c</i>	<i>Pca</i> 2 ₁
<i>a</i> (Å)	9.2107(2)	29.601(3)
<i>b</i> (Å)	8.1173(2)	7.2524(1)
<i>c</i> (Å)	18.133(4)	13.345(2)
α (deg)	90.0(0)	90.0(0)
β (deg)	100.5(1)	90.0(0)
γ (deg)	90.0(0)	90.0(0)
<i>V</i> (Å ³)	1333.04(5)	2865.15(7)
<i>Z</i>	4	8
density calcd (mg/m ³)	4.022	4.655
abs coeff (mm ⁻¹)	27.911	30.137
<i>F</i> (000)	1392	3392
cryst size (mm ³)	0.08 × 0.06 × 0.04	0.15 × 0.10 × 0.10
no. of reflns collected	20973	6261
no. of independent reflns	3054 (R(int) = 0.0540)	6261 (R(int) = 0.00)
refinement method	full-matrix least-squares on <i>F</i> ²	full-matrix least-squares on <i>F</i> ²
GOF on <i>F</i> ²	1.086	1.044
final R indices [<i>I</i> > 2σ(<i>I</i>)]	R1 = 0.0248 wR2 = 0.0427	R1 = 0.0345 wR2 = 0.0740
R indices (all data)	R1 = 0.0366 wR2 = 0.0455	R1 = 0.0429 wR2 = 0.0776
extinction coeff	0.00040(3)	0.00011(2)
largest diff peak and hole (e Å ⁻³)	1.339 and -1.164	2.342 and -2.345

Table 2. Selected Bond Distances (Å) and Angles (deg) for **1**^a

Hg(1)–S(1)	2.518(1)	Hg(2)–S(1) #1	2.473(1)
Hg(1)–S(2)	2.476(1)	Hg(2)–S(2)	2.530(1)
Hg(1)–N(1)	2.404(4)	Hg(2)–N(2)	2.371(4)
Hg(1)–I(1)	2.762(4)	Hg(2)–I(2)	2.755(4)
S(2)–Hg(1)–S(1)	123.47(5)	S(2)–Hg(2)–S(1) #1	124.18(5)
N(1)–Hg(1)–S(1)	81.53(1)	N(2)–Hg(2)–S(1) #1	108.94(1)
N(1)–Hg(1)–S(2)	109.45(1)	N(2)–Hg(2)–S(2)	82.00(1)
S(1)–Hg(1)–I(1)	112.34(4)	S(1) #1–Hg(2)–I(2)	112.35(3)
S(2)–Hg(1)–I(1)	115.81(3)	S(2)–Hg(2)–I(2)	112.65(3)
Hg(1)–S(2)–Hg(2)	104.62(5)	Hg(1)–S(1)–Hg(2) #1	100.62(5)

^a #1 = -*x* + 2, -*y* + 1, -*z*.

for [Hg₄I₈(SCH₂CH₂NH₃)₂]₂·2H₂O: C, 2.392; H, 0.9036; N, 1.395. Found: C, 2.390; H, 0.9032; N, 1.399.

Results and Discussion

Synthesis. The combination of 2-aminoethanethiol and HgI₂ in a 90:10 mixture of water:methanol yielded compounds **1** and **2** in high yield. Methanol was added to increase the solubility of HgI₂, whose solubility is otherwise negligible in water. The precipitates were washed with methanol and cold water to remove excess thiol. Crystals were obtained from partially evaporating filtrate and also from recrystallization of the precipitates from water. A reaction similar to that of **2** also yielded a linear mercury–bis-thiolate, [Hg(SCH₂CH₂NH₃)₂]₂, that is isostructural with [Hg(SCH₂CH₂NH₃)₂]₂Cl₂ (Scheme 1).²¹ The bis-thiolate could be considered as an intermediate en route to **1** or **2**, similar to the observations made for the Hg(II) adduct with L-cysteine (L-CysH), in which the polymeric [HgCl₂(L-Cys)] product in hot water transforms to linear bis-thiolate [Hg(L-Cys)(L-CysH)]⁺.¹⁹ However, for **1** and **2**, a bis-thiolate derivative from hot water could not be isolated (Scheme 1). In contrast, it is likely that the solution rearrangement of the smaller compounds (two- and three-coordinate) leads to the formation of **1** and **2**.

Solution State Studies. The ¹H NMR spectra of **1** and **2** show a significant downfield shift of the methylene protons attached to sulfur (2.84 and 3.04 ppm, respectively) with respect to the free ligand (2.69 ppm). These shifts are, however, slightly upfield compared to those observed for [Hg(SCH₂CH₂NH₃)₂]²⁺ (3.27 ppm), [Hg₆Cl₈(SCH₂CH₂NH₃)₈]⁴⁺ (3.14 ppm), and [Hg₆Br₁₅(SCH₂CH₂NH₃)₉]³⁺ (3.15 ppm). In **1**, the shift observed for the methylene protons adjacent to nitrogen (2.96 ppm) is comparable to that observed in four-coordinate [Hg(SCH₂CH₂NH₂)₂] (2.92 ppm)²⁹ and polymeric [HgCl(SCH₂CH₂NH₂)(H₂O)]_n (2.97 ppm),³⁰ indicating an Hg–N contact. In the ¹³C spectra, a downfield shift is observed for C–S in **1** (29.1 ppm) and **2** (27.3 ppm) with respect to the signal of 2-aminoethanethiol (22.2 ppm).³¹ The C–N peaks, however, do not show profound shifts (42.5 (**1**) and 42.7 ppm (**2**)) from that observed for the free ligand (42.8 ppm for 2-aminoethanethiol). This observation is in contrast to the presence of the Hg–N bond observed in **1**. Similar observation has been made for [HgCl(SCH₂CH₂NH₂)(H₂O)]_n, in which, despite the presence of the Hg–N bond, the shift for the C attached to nitrogen is meager.³⁰ It can be concluded that in the presence of an addition Hg–X bond, the shielding of carbon attached to nitrogen is negligible, something not observed in [Hg(SCH₂CH₂NH₂)₂] (46.1 ppm), in which a significant shift is observed despite a weaker Hg–N bond.²⁹

Attempts were made to obtain ¹⁹⁹Hg NMR spectra of **1** and **2** under similar conditions; however, no detectable peak could be observed for the latter, which might be due to the

(29) Fleischer, H.; Dienes, Y.; Mathiasch, B.; Schmitt, V.; Schollmeyer, D. *Inorg. Chem.* **2005**, *44*, 8087.

(30) Bharara, M. S.; Bui, T. H.; Parkin, S.; Atwood, D. A. *J. Chem. Soc., Dalton Trans.* **2005**, 3874.

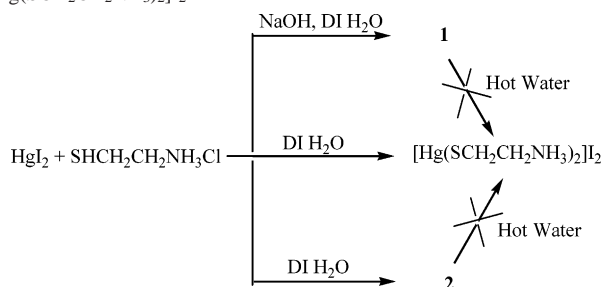
(31) *Spectral Database for Organic Compounds*; SDBS No. 3607 and 3935.

Table 3. Selected bond distances (Å) and angles (deg) for **2**^a

Hg(1)–S(1)	2.464(3)	Hg(2)–S(2)	2.463(3)
Hg(3)–S(1)#1	2.491(3)	Hg(3)–S(2)	2.482(3)
Hg(3)#2–S(1)	2.491(3)	Hg(1)–I(1)	2.936(9)
S(1)–Hg(1)–I(1)	106.21(8)	S(2)–Hg(2)–I(1)	104.09(3)
S(1)–Hg(1)–I(2)	99.50(8)	S(2)–Hg(2)–I(2)	106.77(8)
S(1)–Hg(1)–I(3)	141.62(8)	S(2)–Hg(2)–I(4)	139.56(8)
S(1)#1–Hg(3)–I(5)	98.09(8)	S(1)#1–Hg(3)–I(6)	110.60(8)
S(2)–Hg(3)–S(1)#1	133.59(9)	I(1)–Hg(1)–I(2)91.19(3)	
I(1)–Hg(2)–I(2)92.42(3)		I(1)–Hg(1)–I(3)105.26(3)	
I(1)–Hg(2)–I(4)102.38(3)		I(2)–Hg(1)–I(3)101.26(3)	

^a #1 = x, y + 1, z.

Scheme 1. Reaction Scheme for the Syntheses of **1**, **2**, and [Hg(SCH₂CH₂NH₃)₂]₂



presence of three independent Hg centers and/or a highly shielded environment around Hg. However, using the same parameters, the ¹⁹⁹Hg NMR spectrum of HgI₂ in *d*₆-DMSO could be observed (−3435 ppm).³² For **1**, a single broad peak is observed at −642 ppm, indicating a tetrahedral geometry around Hg. The broadening of the NMR signal supports the presence of an Hg–N bond, because coupling between N and Hg could be responsible for the broadening. Similar broadening has been observed for amine–mercuric chloride complexes²⁴ as well as in [Hg(SCH₂CH₂NH₂)₂] (−659 ppm in *d*₆-DMSO).²⁹ Under the experimental conditions in which the clusters are dissociating into two- and three-coordinate compounds in solution, the chemical shifts usually observed for these compounds in the range δ −1200 to −800 are not observed for either **1** or **2**.⁵

In the UV–vis spectrum (Figure 1) the λ_{max} for both **1** and **2** is observed around 270 nm (ε ≈ 80 000 M^{−1} cm^{−1}), which is due to the S → Hg LMCT. However, low-energy charge-transfer bands in the wavelength range 280–310 nm are characteristic of Hg(II)-thiolates with distorted tetrahedral geometry, as observed in [Hg(SR)₂] (R = Et and Prⁱ),³³ Hg–plastocyanin,³⁴ and two types of metallothionein.³⁵ The presence of an additional Hg–X bond might be responsible for this difference. The compounds seem to retain a tetrahedral geometry around the Hg atoms and do not form two- or three-coordinate complexes. For such lower coordination numbers, the λ_{max} is usually observed in the range 230–250 nm. For **2**, the spectrum contains a shoulder at around 360 nm (ε ≈ 20 000 M^{−1} cm^{−1}). Similar shoulders have been observed in Hg-substituted proteins and [Hg₉Br₁₅(SCH₂CH₂NH₃)₉]³⁺ in the range 280–340 nm and are characteristic of a complicated structure.

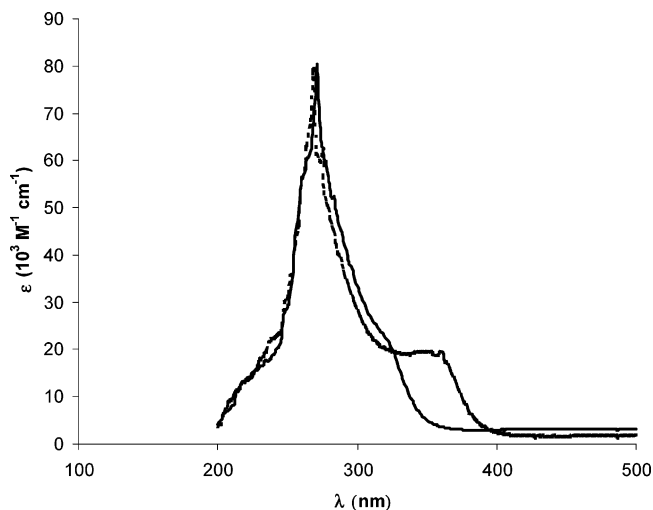


Figure 1. UV–vis spectra of 0.05 mM solutions of **1** (–) and **2** (···) in an 80:20 v/v water:DMSO mixture.

Solid State Studies. The IR spectra for both **1** and **2** are quite similar to that of the free ligand except for the missing SH peak around 2500 cm^{−1}. A significant change in the C–S stretch for **1** and **2** (≈629–675 cm^{−1}) is observed (free ligand = 757 cm^{−1}). This might be due to the slight difference in the C–S distance in **1** and **2** compared to that in the free ligand, as evident from the X-ray studies. Peaks around 3000–3448 cm^{−1} in **1** can be assigned to antisymmetric as well as symmetric NH₂ stretches, which are characteristic of primary amines. In **2**, the band at 2962 cm^{−1} can be assigned to a symmetric NH₃⁺ stretch. Also, peaks at 1468 and 1594 cm^{−1} can be assigned to symmetric deformation and degenerate deformation modes, respectively, for the NH₃⁺ group. Similar peaks have been observed for mercury compounds with L-cysteine (1487 and 1606 cm^{−1}) and L-cysteine methyl ester (1495 and 1582 cm^{−1}).³⁶

In the Raman spectrum for **1**, the symmetric and asymmetric frequencies for Hg–S are observed at 260 and 341 cm^{−1}, respectively. In **2**, the corresponding peaks are observed around 287 and 340 cm^{−1} and are in the range observed for a distorted tetrahedral Hg environment. In **1**, the peak observed at 499 cm^{−1} can be assigned to the Hg–N stretch, which is in the range observed for Hg-thiolate with Hg–N bonding (400–700 cm^{−1}).³⁷ The terminal Hg–I frequencies for both **1** and **2** can be assigned to the peaks at

(32) Goodfellow, R. J. *Multinuclear NMR*; Plenum Press: New York, 1987.

(33) Watton, S. P.; Wright, J. G.; MacDonnell, F. M.; Bryson, J. W.; Sabat, M.; O'Halloran, T. V. *J. Am. Chem. Soc.* **1990**, *112*, 2824.

(34) Tamilarasan, R.; McMillin, D. R. *Inorg. Chem.* **1986**, *25*, 2037.

(35) Beltramini, M.; Lerch, K.; Vasak, M. *Biochemistry* **1984**, *23*, 3422.

(36) Sze, Y. K.; Davis, A. R.; Neville, G. A. *Inorg. Chem.* **1975**, *14*, 1969.

(37) Nakamoto, K. *Infrared Spectra of Inorganic and Coordination Compounds*; Wiley: New York, 1963.

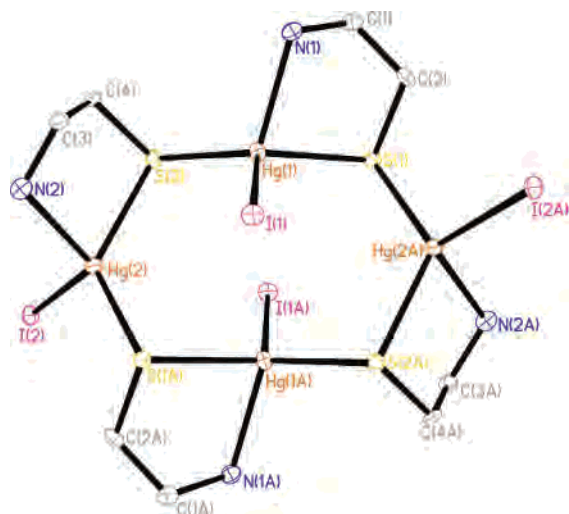


Figure 2. View of **1** with 50% probability level thermal ellipsoids; hydrogen atoms are omitted for clarity.

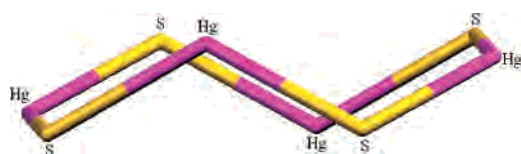


Figure 3. Chair configuration acquired by the core of **1**.

127 and 133 cm^{-1} , respectively, and are in accord with the terminal Hg–I frequencies reported in the literature.^{16,18,38} The peak at 106 cm^{-1} in **2** can be assigned to the bridging Hg–I stretch, which is comparable to the peak observed in $[\text{Hg}_2\text{I}_6]^{2-}$.³⁹

Crystal Structures. Compound **1** contains a centrosymmetric tetranuclear molecule with an eight-membered ring consisting of alternate Hg and S atoms. The four metal centers have similar coordination environments consisting of S, N, and a terminal I atom (Figure 2). The octagonal ring is nonplanar, with the I atoms attached to Hg and present on opposite sides of the mean plane. However, the geometry defined by the four Hg atoms can be considered as being square planar, with S atoms present above and below the plane. The sets of equivalent $[\text{HgI}(\text{SCH}_2\text{CH}_2\text{NH}_2)]$ units are connected through bridging S atoms. In a similar structure, $[\text{Hg}_4\text{Cl}_4(\text{SCH}_2\text{CH}_2\text{N}(\text{CH}_3)_2)_4]$ (**3**), the tetranuclear units are also composed of two independent Hg centers, namely HgS_2N_2 and HgS_2X_2 ($\text{X} = \text{Cl}$ or Br).¹⁰ The geometry around HgS_2Cl_2 is distorted tetrahedral, whereas that around HgS_2N_2 is close to octahedral with secondary interactions with Cl or Br ions.

In **1**, the absence of a $[\text{HgS}_2\text{I}_2]$ unit can be attributed to the use of base as well as steric effects exerted by the much larger iodide ions. The Hg_4S_4 core (Figure 3) can also be viewed as consisting of an Hg_2S_2 plane with an additional HgS on each side of the plane, achieving a relaxed chair configuration.

The geometry around the Hg atoms is distorted tetrahedral, with the smallest angles observed in the five-membered ring

($\text{N}-\text{Hg}-\text{S} \approx 82^\circ$) and the largest angles associated with the thiolate S atoms ($\text{S}-\text{Hg}-\text{S}' \approx 123^\circ$) (Table 2). Similar observations were also made in the case of **3**, with $\text{N}-\text{Hg}-\text{S} \approx 81^\circ$ and $\text{S}-\text{Hg}-\text{S} \approx 163^\circ$. The lesser distortion of the S–Hg–S angle in **1** can be attributed to the absence of secondary contacts, something that is observed in **3**. The Hg1–S1 distance (2.518 Å) associated with the five-membered S/N chelate is longer than the bridging Hg1–S2 distance (2.476 Å), which is contrary to the corresponding distances in **3** (2.415 and 2.487 Å, respectively). However, the difference in the asymmetric bonds is much smaller in **1** (0.042 Å) compared to that observed in **3** (0.072 Å), which might be due to the much larger difference in donor strength between I and S compared to that between Cl and S.¹⁸

The Hg1–S1 distance is similar to the sum of the covalent radii of tetrahedral Hg and S atoms (2.52 Å), whereas Hg2–S1 is much smaller.⁴⁰ Asymmetrical distances are quite common for Hg–thiolates, in which formation of a longer bond is compensated by the presence of another shorter Hg–S bond to achieve overall stability.⁴¹ These distances are, however, smaller than Hg–thiolates containing the $[\text{Hg}(\text{SR})_x\text{I}_2]$ moiety, in which longer Hg–S bonds are observed because of the presence of two stronger Hg–I contacts ($\text{SR} = (1,3\text{-thiazolidine-2-thione})_2$ (2.67–2.68 Å),⁴² $(\text{SCHN}(\text{CH}_3)_2)_2$ (2.57–2.58 Å),¹⁸ and 1-(methyl-imidazoline-2(3H)-thione)₂ (2.52–2.57 Å)).¹⁷ The Hg–N distances are variable (2.371 and 2.404 Å) but in accordance with the corresponding distances observed in Hg(II)-thiolates with an additional N donor ligand, such as in $[\text{HgO}_2\text{CCH}_2(\text{RS})(\text{L})]$ ($\text{R} = \text{Me}$, Et , and $\text{L} = \text{C}_6\text{H}_7\text{N}$ and $\text{C}_5\text{H}_5\text{N}$; avg Hg–N = 2.48 Å)^{11,43} and $[\text{Hg}(\text{Am4DM})\text{X}]_2$ ($\text{Am4DM} = 2\text{-pyridine-formamide N(4)-dimethylthiosemicarbazone}$; avg Hg–N = 2.393 Å).¹⁵ It can be concluded that in Hg–thiolates, the Hg–N interactions do not contribute to the structural variability in comparison to the halides. The Hg–I distance (2.759 Å) is shorter than the sum of covalent radii of tetrahedral Hg and I (2.81 Å) and comparable to Hg(II)-thiolates with similar bonding patterns, such as $[(\mu\text{-I})(\mu\text{-SP}^n)(\text{HgI}_2)_2]^{2-}$ (2.727 Å) and $(\text{C}_{18}\text{H}_{26}\text{N}_2\text{S}_2)[\text{HgI}_4]$ (2.782 Å).¹⁴

A mechanistic pathway for the formation of **1** in solution can be proposed. The three-coordinate intermediate $[\text{Hg}(\text{S}/\text{N})\text{I}]$, reported for several S/N chelate Hg complexes,^{44,45} could not be isolated, despite the TGA and mass spectrometry data. The formation of this intermediate is most likely due to the partial solubility of HgI_2 in water, which otherwise in alcohol would have yielded $[\text{Hg}(\text{S}/\text{N})_2]^{29}$ or $[\text{Hg}(\text{S}/\text{N})\text{I}_2]$. The four-coordinate $[\text{Hg}(\text{S}/\text{N})_2]$ can be obtained by the use of base and 2-aminoethanethiol hydrochloride in alcohol regardless of the type of Hg(II) salt. The stability of the three-

(40) Grdenic, D. *Q. Rev., Chem. Soc.* **1965**, *19*, 303.

(41) Gruff, E. S.; Koch, S. A. *J. Am. Chem. Soc.* **1990**, *112*, 1245.

(42) Popovic, Z.; Pavlovic, G.; Soldin, Z.; Popovic, J.; Matkovic-Calogovic, D.; Rajic, M. *Struct. Chem.* **2002**, *13*, 415.

(43) Canty, A. J.; Raston, C. L.; White, A. H. *Aust. J. Chem.* **1978**, *31*, 677.

(44) Veveris, O.; Bankovskii, Y. A.; Pelne, A. *Latv. PSR Zinat. Akad. Vestis, Kim. Ser.* **1975**, *4*, 451.

(45) Zuiika, I.; Bankovskii, Y. A.; Borodkin, Y. G. *Russ. J. Coord. Chem.* **1979**, *5*, 1765.

(38) Bell, N. A.; Branston, T. N.; Clegg, W.; Parker, L.; Raper, E. S.; Constable, C. P.; Sammon, C. *Inorg. Chim. Acta* **2001**, *319*, 130.

(39) Svensson, P. H.; Kloo, L. *Inorg. Chem.* **1999**, *38*, 3390 and refs therein.



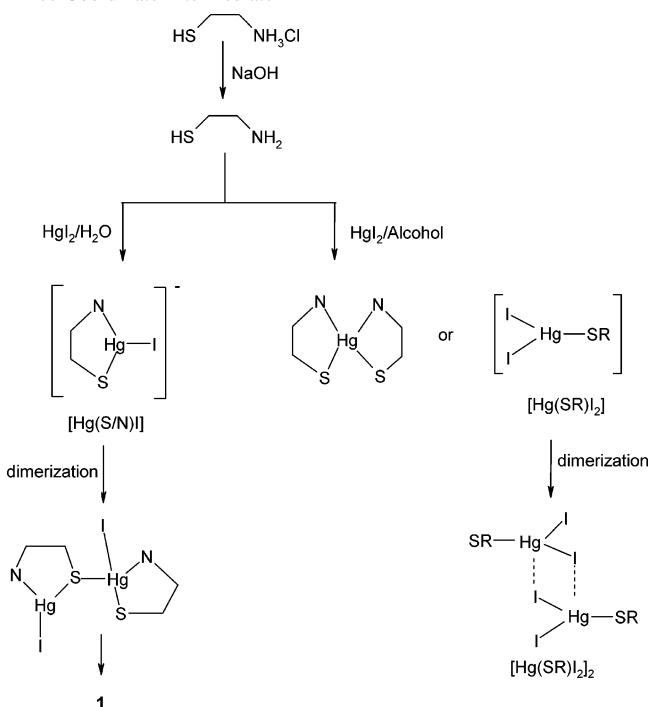
Figure 4. One-dimensional chain of **2** (at 50% probability level thermal ellipsoids) showing bridging Hg–S contacts.

coordinate intermediate is achieved by dimerization, yielding a tetrahedral geometry around Hg. For instance, a dimer $[Hg(S/N)I_2]_2$ is observed for $[Hg(S/N)I_2]$, as observed for **2**. However, the choice of formation of $[Hg(S/N)I(\mu-S)]$ over $[Hg(S/N)I_2]_2$ is due to the preference of Hg for S over I (bond energies 217.1 and 34.69 kJ/mol, respectively). This is also evident from the X-ray structure, in which the Hg–S distance between two $[Hg(S/N)I]$ units is longer than that in the five-membered ring.

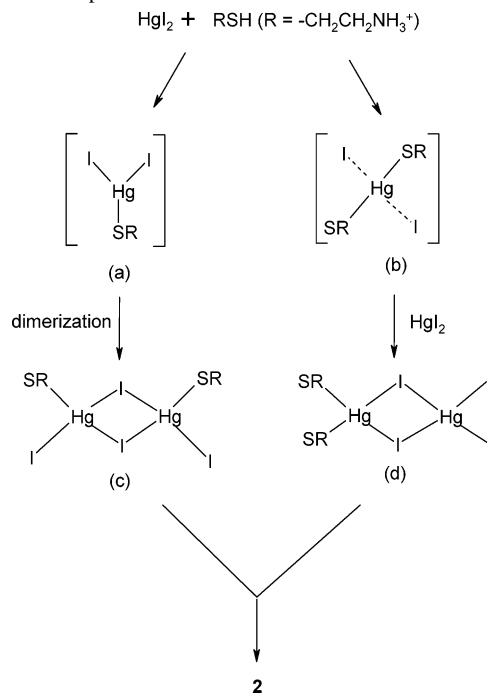
The tetranuclear repeating unit in **2**, $[Hg_4I_8(SCH_2CH_2NH_3)_2] \cdot 2H_2O$, consists of three independent Hg centers, namely HgI_3S , HgI_2S_2 , and HgI_4 , and is connected through bridging S atoms to form a one-dimensional polymeric chain (Figure 4).

$Hg1$ and $Hg2$ are quite similar and bonded to one bridging S, one terminal I, and two bridging I atoms; $Hg2$ is bonded to two bridging S and I atoms, and $Hg4$ is attached to two bridging and two terminal I atoms. $Hg4$ is quite unique in being coordinated to four I atoms. A similar HgX_4 unit is observed in $[Hg(C_4H_4N_2S)(C_4H_3N_2S)]_2[HgBr_4]$, in which the $[HgBr_4]$ unit is only weakly bonded to the $[Hg(C_4H_4N_2S)(C_4H_3N_2S)]_2$ unit. The geometry around all the Hg atoms can be best described as distorted tetrahedral, which is indicated by angles ranging from 141 to 89°. The smallest range is observed in the HgI_4 moiety followed by the HgI_3S unit, which suggests the tendency of Hg to maximize bonding with S ($S-Hg-S = 133.5^\circ$ in the HgS_2I_2 moiety). Similar trends have been observed in polymeric structures such as $[HgCl_2\{L-CysH\}]$ ($S-Hg-S = 136^\circ$ and $Cl-Hg-Cl = 91.4^\circ$) and $[HgCl_2\{\mu-S(CH_2)_3NH(CH_3)_2\}]$ ($S-Hg-S = 130.2^\circ$ and $Cl-Hg-Cl = 99.0^\circ$).¹⁰ The $Hg-I_{\text{bridging}}-Hg$ angles observed (avg 86.7°) are in the range found for $Hg_2I_6^{2-}$ (83.8–88.0°) but larger than those observed in $(Et_4N)_2[(\mu-I)(\mu-SC_3H_7)(HgI)_2]$ (**4**) (74.9°).^{14,46} Also, the $Hg-S-Hg$ angles (avg 105.5°) are much larger than those reported for **4** (90.2°) and $[(MeS)_2Hg(SMe)_2Hg(SMe)_2]^{2-}$ (85.7°).⁶ The Hg–S distances in the tetranuclear unit as well as those between the repeating units (avg 2.478 Å) are in accordance with polymeric heteroleptic Hg-thiolates (avg 2.471,¹⁹ 2.431,⁷ and 2.464 Å).¹⁰ Selected bond distances and angles are summarized in Table 3. The Hg–I distances are variable depending on their presence at terminal (avg 2.687 Å) or bridging (avg 2.953 Å) positions; the distances are also in agreement with corresponding distances observed in

Scheme 2. Proposed Mechanism for the Formation of **1** through a Three-Coordinate Intermediate



Scheme 3. Proposed Mechanism for the Formation of **2**



Hg-thiolates with both terminal and bridging Hg–I bonding, such as $[HgI_2(tzdtH)]_2$ ($tzdtH = 1,3$ -thiazolidine-2-thione; 2.669 Å (ter) and 3.059 Å (br)) and $[Hg_2I_5(SC_3H_7)]^{2+}$ (2.723 Å (ter) and 2.994 Å (br)).¹⁴

On the basis of two distinct $Hg_2S_2I_4$ moieties and common features observed for HgI_2 -thiolates, we can propose a general mechanism for the formation of **2** (Scheme 3). The combination of HgI_2 with thiol forms two types of structures with $HgSI_2$ (a) and HgS_2I_2 (b) units. The square planar $[Hg(SCH_2CH_2NH_3)_2]I_2$ (b), also obtained by the direct combination of reactants, exists as a four-coordinate complex

(46) Fabry, J.; Maximov, B. A. *Acta Crystallogr., Sect. C: Cryst. Struct. Commun.* **1991**, *47*, 51.

with [2+2] in solution ($\lambda_{\max} \approx 270$ nm). This intermediate then comes in contact with an additional HgI_2 and forms an $\text{Hg}_2\text{S}_4\text{I}_4$ unit (d). On the other hand, the three-coordinate moiety, HgSI_2 (observed for HgI -thiolates containing relatively larger ligands such as 1,3-thiazolidine-2-thione⁴² and 1,3-imidazole-2-thione⁴⁷), rearranges to form a dinuclear species (c), as proposed in Scheme 2. The three-coordinate (a) or dinuclear (c) species could be isolated from less polar solvents, for which the rate of ligand exchange is much slower. The molecules in **1** and **2** are connected through intermolecular hydrogen bonding, forming a three-dimensional network. These intermolecular contacts might be responsible for the nonplanar octagonal ring observed in **1**. Because of the stronger $\text{Hg}-\text{I}$ bonds, the $\text{NH}\cdots\text{I}$ distances in **1** (avg 3.807 Å) and **2** (avg 3.78 Å) are longer than those observed in $[\text{HgI}_2(\text{SR})]$ type compounds (SR = benzo-1,3-imidazole-2-thione (avg = 3.69 Å), 1-methyl-imidazoline-2(3H)-thione (avg = 3.593 Å)). The $\text{NH}\cdots\text{O}$ distance in **2** (2.85 Å) is comparable to the value cited in the literature (2.840 Å).⁴⁸ The $\text{NH}\cdots\text{S}$ distances observed in **1** (avg 3.442 Å) are in the lower range of those observed for tetrahedral $\text{Hg}(\text{II})$ complexes with similar interactions (3.398–3.733 Å).^{42,49} It is quite interesting to observe that only N2 is involved with S, whereas N1 is involved with only I. This might be due to the orientation of the molecules in the packing structure. Such selective interactions are, however, not observed in **2**. The shortest $\text{Hg}\cdots\text{Hg}$ distances in **1** (3.841 and 3.962 Å) and **2** (3.938 and 4.049 Å) do not indicate mercurophilic interaction but are in agreement with those observed in $[\text{Hg}(\text{SR})\text{X}]$ type compounds such as $[\text{Hg}(\text{Am4DM})\text{X}]_2$ (Am4Dm = 2-pyridineformamide N(4)-dimethylthiosemicarbazone and X = Cl or Br; 3.667 and 3.660 Å)¹⁵ and $[(\text{Bu}^t\text{S})_4\text{Cl}_4\text{Hg}_4(\text{C}_6\text{H}_7\text{N})_2]$ (3.648–3.852 Å).^{11,43}

TGA Studies. The thermogram of **1** in the presence of air shows that the total degradation of the sample takes place stepwise, similar to what was observed in similar compounds.⁵⁰ The removal of one molecule of $[\text{HgI}(\text{SCH}_2\text{CH}_2\text{NH}_2)]$ accounts for 24% loss, which is close to the theoretical value of 25%. In the second step, the remaining $[\text{Hg}_3\text{I}_3(\text{SCH}_2\text{CH}_2\text{NH}_2)_3]$ degrades to form HgS , accounting for 60% loss, which is comparable to the calculated value of 60.5%. The thermogram of **2** is quite interesting, as it is observed that



Figure 5. Two distinct structural motifs of $\text{Hg}_2\text{I}_4\text{S}_4$ type are observed in compound **2**. The $\text{CH}_2\text{CH}_2\text{NH}_3\text{Cl}$ group attached to S is not shown.

total degradation of the sample takes place around 600 °C with most of the weight loss occurring in a single step ($\approx 98\%$ loss to form HgS). The distinct profile of **2** can be correlated to the presence of fewer $\text{Hg}-\text{S}$ than $\text{Hg}-\text{I}$ contacts. Compound **2** may be considered as being a potential precursor to solid-state materials.

Conclusion

In this study, novel HgI -thiolates were characterized in solution and solid state, with a possible mechanism proposed for the formation of clusters through more simple units. It is observed that the stronger $\text{Hg}-\text{I}$ contacts lead to the formation of low-coordinate compounds, which serve as a precursor for thiolate clusters. On the other hand, Hg -thiolates with $\text{Hg}-\text{X}$ (X = Cl, Br) contacts along with additional secondary contacts are more prone to undergo rearrangement in solution. It can also be argued that, in solution, the rearrangement of $\text{Hg}(\text{II})$ -thiolate clusters is less feasible compared to lower-coordination molecular complexes (2, 3, or 4), which makes their solution studies more complicated.

Acknowledgment. This work was supported by the University of Kentucky Tracy Farmer Center for the Environment and with partial support from the Center for Applied Energy Research Center Fund. NMR instruments used in this research were obtained with funds from the CRIF program of the National Science Foundation (Grant CHE 997841) and from the Research Challenge Trust Fund of the University of Kentucky.

Supporting Information Available: Syntheses, characterization information, additional figure, extensive tables, thermograms, ¹⁹⁹Hg NMR of **1**, and crystal data. Crystallographic data for the structures analysis for compounds **1** and **2** have been deposited with the Cambridge Crystallographic Data Center, CCDC No. 273880 and 273881, respectively. Copies of information may be obtained free from the Director, CCDC, 12 Union Road, Cambridge CB2 1EZ, UK (phone: 44 1223 336408; fax: 44 1223 336033). This material is available free of charge via the Internet at <http://www.pubs.acs.org>.

IC051993A

(47) Popovic, Z.; Matkovic-Calogovic, D.; Soldin, Z.; Pavlovic, G.; Davidovic, N.; Vikić-Topić, D. *Inorg. Chim. Acta* **1999**, *294*, 35.

(48) Steiner, T. *Angew. Chem., Int. Ed.* **2002**, *41*, 48.

(49) Popovic, Z.; Soldin, Z.; Matkovic-Calogovic, D.; Pavlovic, G.; Rajić, M.; Giester, G. *Eur. J. Inorg. Chem.* **2002**, 171.

(50) Faraglia, G.; Guo, Z.; Sitran, S. *Polyhedron* **1991**, *10*, 351.